Journal of Imaging Science and Technology® 56(1): 010504-1–010504-8, 2012.

Dependence of Electrostatic Field Strength on Image Transfer Roller Dimensions in a Toner Transfer Region

Julijonas Kaladė and Robertas Maldzius
Department of Solid State Electronics, Vilnius University, Sauletekio av. 9, LT-10222 Vilnius, Lithuania
E-mail: robertas.maldzius@ff.vu.lt

Jonas Sidaravicius
Department of Polygraphic Machines, Vilnius Gediminas Technical University, J. Basanavicius str. 28, LT-03224, Lithuania

Petri Sirviö
Stora Enso Oyj, Imatra Research Centre, FI-55 800 Imatra, Finland and Department of Physical Chemistry, Åbo Akademi University, Porthaninkatu 3-5, FI-20 500 Turku, Finland

Kaj Backfolk▲
Laboratory of Fibre and Paper Technology, Lappeenranta University of Technology, FI-53 851 Lappeenranta, Finland

Abstract. *Using an expansion of electrostatic potential in terms of partial solutions of the Poisson equations, a distribution of electrostatic field strength in a two-dimensional (2D) toner transfer system region between the toner and the paper has been calculated. The results have been obtained for a system in which photoreceptor and toner transfer element is a roller with a finite radius. In these calculations, the photoreceptor, the toner, and the paper have been characterized by the values of their thickness and dielectric permittivity. Results have been obtained when the transfer element is flat and when it is shaped as a roller with a finite radius. It is concluded that the one-dimensional (1D) approximation cannot be applied to calculate the electric field when the roller radius is close to or less than the radius of the cylinder-shaped photoreceptor. The limits of applicability of the dielectric thickness have been demonstrated.*

[DOI: 10.2352/J.ImagingSci.Technol.2012.56.1.010504]

INTRODUCTION

The problems of toner image transfer in electrophotographic printers and copiers have been studied by various researchers. The quality of the toner image transferred to the paper or onto the intermediate belt depends on the electric field strength and on its configuration in the image transfer region. Since the real image transfer system is relatively complex (Figure 1) and since the paper is dielectrically inhomogeneous[1–3] with a rough surface profile,[1,4] the mathematical description of charged toner particle transfer is relatively complex. For this reason, the mathematical analysis of the image transfer phase is based on certain simplified models and assumptions. The one-dimensional (1D) approximation to describe the image transfer process is quite common.[5–7] If the image is transferred onto a flat intermediate belt or if the toner image transfer element is flat, the vertical electric field component perpendicular to the paper surface (or the belt) can be accurately described using the 1D approximation model.[8] However, this approximation cannot be used to estimate the horizontal component of the electric field parallel to the paper surface, which can affect the quality of the transferred image. Moreover, if the toner image is transferred using a roller with a radius less than or close to the radius of the cylindrical photoreceptor, neither the vertical component nor the horizontal component of the electric field in the region between the toner and the paper can be calculated using the 1D approximation. In Refs. 9–14, the electric field strength was calculated in a finite 2D region by applying the finite-difference method to solve the Poisson equation. In a real image transfer system, at least some of the regions are infinite (such as the air regions in Fig. 1). After selecting a small region in an infinite or a sufficiently large region, additional problems arise related to the uniqueness of this selection and the boundary conditions of the selected region. Since electrophotographic printers, especially the color ones, have to meet increasingly strict quality requirements, the theoretical predictions to the toner image transfer characteristics must be based on models that are more adequate for the real system geometry and less reliant on additional assumptions.

The electric field distribution in the toner transfer region, when the toner image transfer element is flat and the paper is defined in terms of the dielectric thickness approximation, was calculated by Kaladė et al.[8] The solution of the Poisson equation for the potential in a chosen region of the toner image transfer system is expressed as a

▲IS&T Member.

Received Jun. 28, 2011; accepted for publication Dec. 20, 2011; published online Mar. 14, 2012.
1062-3701/2012/56(1)/010504/8/$20.00.

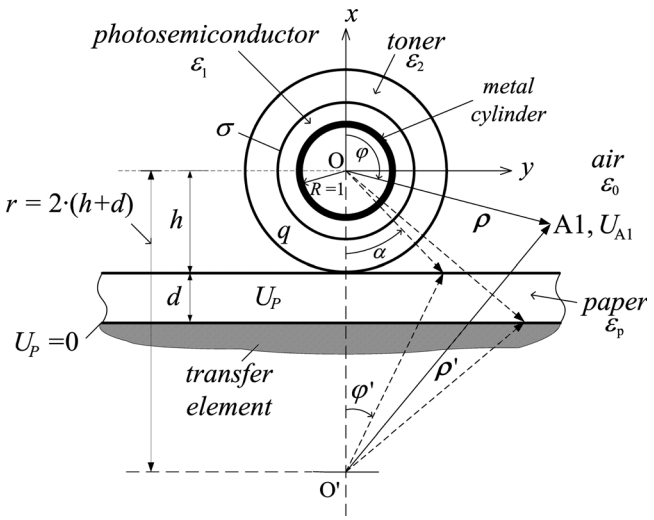

Figure 1. Diagram of the toner image transfer system and definition of the coordinate system in the case of a flat transfer element. The distances ρ and ρ' are the same as in Eq. (5), for other denotations see text.

linear combination of the partial solutions of the Poisson equation for that particular region. The coefficients of this linear combination are calculated from the boundary conditions for the potential on the electrodes and on the interfaces between the different materials. This is an accurate method of potential calculation, both in a finite region and in an infinite region.

This work presents a development of the technique described by Kaladė et al.,[8] with a calculation of the electric field distribution for a system that is more representative of a real electrophotographic image transfer system. In such a device, the toner image is often transferred to the paper using a cylinder-shaped element, so that the geometry of the system and the potential boundary conditions are more complex than in the 1D models or in the case described in Ref. 8. As a result, the problem of calculating the electric field strength is also more complex. For the purpose of investigating the dependence of electrostatic field strength on the transfer roller radius and other system parameters, the paper has been characterized by its thickness and dielectric permittivity separately instead of using the dielectric thickness as in previous work.[8] The paper is considered as dielectric. This assumption is not valid in all cases but it must be noted that in many cases especially in the higher speed printers the Maxwell relaxation time of papers is higher than toner transfer time. Then our approach is reasonable. The initial conditions of the Paschen effect have been discussed. The results obtained may be important for defining the initial toner charge transfer conditions and for evaluating the results obtained using simplified models. The potential calculation method can also be applied under conditions of charge transfer. In the latter case, the coefficients in the expansion of the potential are expressed in the shape of static equations, but these equations correspond to a charge distribution at a particular moment in time instead of a static charge distribution.

The calculation algorithm has been written for the computer programs MATHCAD14 and MATHEMATICA7. The coefficients of the series expansions are integrals of trigonometric functions. The latter functions are also approximated as series in the programs. Hence, an especially important property of the programs is calculation error control. The use of two programs makes it possible to determine calculation errors independently and thus to avoid distortions of the potential distribution curves (oscillations, etc., see Fig. 5 of Ref. 15).

THE MAIN EQUATIONS

Case A. First, let us consider the case when the paper is transported by a flat device and the paper is characterized by its dielectric permittivity ε_p and thickness d separately, instead of using the dielectric thickness d / ε_p as was done in Ref. 8. A diagram of the analyzed system and the coordinates is shown in Fig. 1. The z axis of the coordinate system is directed along the cylinder axis away from the reader. It is assumed that the system is 2D, i. e., homogeneous and infinite in the z-direction, and that the paper and the transporter (flat transfer element) are infinite in the y-direction. It is also assumed that the charges of the photoreceptor and the toner are distributed symmetrically about the xOz plane. The cylinder upon which the photoreceptor is placed is characterized by the potential U_0 and radius R, and the potential of the paper-transporting device is zero. Later, dimensionless quantities will be used, unless otherwise indicated; the potentials being expressed in units of U_0, and dimensions (thicknesses, distances, etc.) in units of R. Using this convention, the cylinder potential and its radius are equal to 1. The electric field strength is expressed in units of U_0 / R.

Under the above symmetry conditions, the distribution of potential U in polar coordinates in any region of the analyzed system is described by the following equation:

$$\frac{\partial^2 U}{\partial \rho^2} + \frac{1}{\rho}\cdot\frac{\partial U}{\partial \rho} + \frac{1}{\rho^2}\cdot\frac{\partial^2 U}{\partial \varphi^2} = -Q, \tag{1}$$

where ρ is the polar vector, φ is the angle, and Q is the dimensionless space charge density,

$$Q = qR^2 / \varepsilon_a U_0, \tag{2}$$

where q is the dimensional (C/m^3) space charge density, and ε_a is the dielectric permittivity of the region. The partial solutions of the homogeneous equation (1) are

$$\text{Const}, \quad \ln\rho, \quad \rho^n \cos(n\cdot\varphi), \quad \rho^{-n}\cos(n\cdot\varphi), \quad n = 1, 2, \ldots, \tag{3}$$

The partial solution of the inhomogeneous equation in the case of constant Q is

$$U_q = -\frac{1}{4} Q\rho^2. \tag{4}$$

The general solution of Eq. (1) is a linear combination of all or some of partial solutions.

In order to make it mathematically easier to satisfy the potential boundary conditions, the electrostatic potential in the air region between the toner and the paper (Fig. 1, region A1) is expressed in terms of partial solutions of two centers, as in Ref. 8, i. e.,

$$U_{A1} = B\ln\frac{\rho}{\rho'} + \sum_{n=1}^{\infty}\left(C_n\frac{\cos n\varphi}{\rho^n} + D_n\frac{\cos n\varphi'}{\rho'^n}\right), \quad (5)$$

where ρ' is measured from the point O′ (Fig. 1), which is the mirror reflection of the coordinate origin O (located on the cylinder axis) in the bottom surface of the paper. The distance between O and O′ is equal to $r=2\cdot(h+d)$. B, C_n, D_n are the expansion coefficients, which are determined from the potential boundary conditions.

The investigated region extends an arbitrarily distance from O and O′, and Eq. (5) has, therefore, been formulated using only those partial solutions and their linear combinations that vanish when the distance from O and O′ tends to infinity. If the photoreceptor and/or toner charges were not symmetrical about the xOz plane, Eq. (5) would include terms proportional to sin $n\varphi$ and sin $n\varphi'$.

The paper electrostatic potential U_P is expressed in terms of the same coordinates as U_{A1},

$$U_P = B_P\ln\frac{\rho}{\rho'} + \sum_{n=1}^{\infty}\left(C_{Pn}\frac{\cos n\varphi}{\rho^n} + D_{Pn}\frac{\cos n\varphi'}{\rho'^n}\right). \quad (6)$$

The bottom surface of the paper ($x=-h-d$) must satisfy the condition $U_P=0$. Taking into account that $\rho'=\rho$, cos $n\varphi'=(-1)^n$ cos $n\varphi$ ($\varphi'=\pi-\varphi$) on any point of that surface, it is found that the condition $U_P=0$ is automatically satisfied, if

$$D_{Pn} = (-1)^{n+1}C_{Pn}. \quad (7)$$

Assuming that there are no charges on the top surface of the paper ($x=-h$), the following boundary conditions are satisfied:

$$U_{A1}|_{x=-h} = U_P|_{x=-h}, \quad \frac{\varepsilon_0}{\varepsilon_P}\frac{\partial U_{A1}}{\partial x}\bigg|_{x=-h} = \frac{\partial U_P}{\partial x}\bigg|_{x=-h}, \quad (8)$$

where ε_P is the paper dielectric permittivity. Since both sides of Eq. (8) are functions of the coordinate y, we can express y via the cosine of the angle α (Fig. 1). Later, the functions of Eq. (8) are expanded in series of cosines of the angle α and the corresponding coefficients in those expansions are set equal to each other. This leads to the relations between the coefficients in Eqs. (5) and (6).

On the toner surface, the air potential U_{A1} and the toner potential U_T are related as follows:

$$U_{A1}|_{\rho=h} = U_P|_{\rho=h}, \quad \frac{\varepsilon_0}{\varepsilon_P}\frac{\partial U_{A1}}{\partial \rho}\bigg|_{\rho=h} = \frac{\partial U_T}{\partial \rho}\bigg|_{\rho=h}. \quad (9)$$

Assuming that there is no space charge in the photoreceptor and that the toner space charge is constant, U_T is obtained in the usual way and is expressed as a series of cosines of the angle φ.[8]

$$\begin{aligned} U_T(\rho,\varphi) = 1 &+ \frac{1}{4}Q\left(\rho_1^2 - \rho^2 - 2h^2\frac{\varepsilon_2}{\varepsilon_1}\ln\rho_1\right) \\ &+ \left(\frac{\varepsilon_2}{\varepsilon_1}\ln\rho_1 + \ln\frac{\rho}{\rho_1}\right)B \\ &+ \sum_{n=1}^{\infty}A_n\left(\frac{\alpha_n}{\rho^n} + \beta_n\frac{\rho^n}{\rho_1^{2n}}\right)\cos n\varphi, \end{aligned}$$

where $\rho_1\le\rho\le h$, $0\le\varphi\le\pi$,

$$\begin{aligned} \alpha_n &= \frac{1}{2}\left(1 + \frac{\varepsilon_2}{\varepsilon_1} - \left(1 - \frac{\varepsilon_2}{\varepsilon_1}\right)\rho_1^{2n}\right) \\ \beta_n &= \frac{1}{2}\left(1 - \frac{\varepsilon_2}{\varepsilon_1} - \left(1 + \frac{\varepsilon_2}{\varepsilon_1}\right)\rho_1^{2n}\right), \end{aligned} \quad (10)$$

where B, A_n are constants, and the other notations are explained in Fig. 1. By similarly expanding the left-hand sides of Eq. (9) and equating the corresponding coefficients on the two sides of these equations, we obtain the relations between the toner potential coefficients and the air potential coefficients. These equations, together with the previously mentioned ones, form a closed system of equations for the determination of the coefficients in the potential expressions.

The results of the calculations of electrostatic field strength in the region between the toner and the paper obtained using this method are presented in Fig. 3. The results have been obtained assuming that the surface charge density on the interface between the photoreceptor and the toner does not depend on the angle φ and that there is a complete mutual compensation between the surface charge and the space charge of the toner.

Case B. Let us now consider the case where the transfer element is a roller with a finite radius ρ_2 and the surface potential is equal to zero. In this case, there are four regions whose potentials are related to each other. The expressions for the toner potential U_T, the potential U_{A1} in the region between the toner and the paper, and the paper potential U_P are exactly the same as in case A. However, Eq. (7) is no longer valid, and the coefficients C_{Pn} and D_{Pn} no longer depend upon each other.

In the air between the bottom paper surface and the roller (Figure 2, region A2), the potential U_{A2} is expressed as follows:

$$U_{A2} = B_A\ln\frac{\tilde\rho}{\tilde\rho'} + \sum_{n=1}^{\infty}\left(C_{An}\frac{\cos n\tilde\varphi}{\tilde\rho^n} + D_{An}\frac{\cos n\tilde\varphi'}{\tilde\rho'^n}\right), \quad (11)$$

where $\tilde\rho$ is measured from the roller axis point $\tilde{\text{O}}$ and $\tilde\rho'$ is measured from the point $\tilde{\text{O}}'$, which is the mirror reflection of the point $\tilde{\text{O}}$ in the bottom surface of the paper ($x=-h-d$), as shown in Fig. 2.

The boundary conditions that must be satisfied on the bottom surface of the paper (assuming that there are no charges on the surface) are the following:

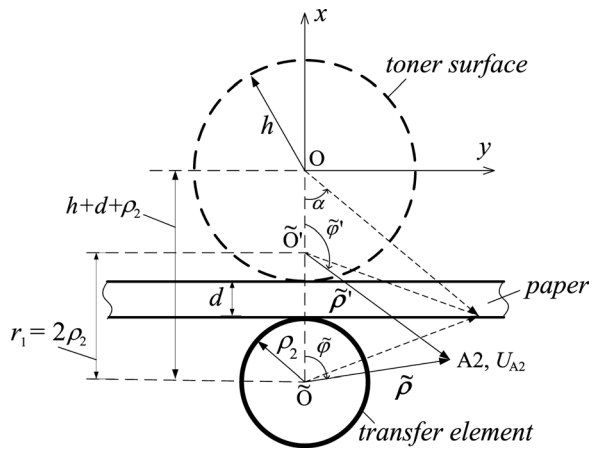

Figure 2. The coordinate system for the determination of the potential U_{A2} in the air between the paper and the roller.

$$U_P|_{x=-h-d} = U_{A2}|_{x=-h-d}, \quad \left.\frac{\partial U_P}{\partial x}\right|_{x=-h-d} = \frac{\varepsilon_0}{\varepsilon_P}\left.\frac{\partial U_{A2}}{\partial x}\right|_{x=-h-d}, \tag{12}$$

Here, as in Eq. (8), both sides of the equations are functions of the coordinate y. By expressing y via the cosine of the angle α (Fig. 2) and then expanding both sides of Eqs. (12) in Fourier series and equating the Fourier coefficients, the relations between the coefficients of U_P and U_{A2} are obtained.

At the points on the roller surface where $\tilde{\rho} = \rho_2$, the potential U_{A2} obeys the equation,

$$U_{A2}|_{\tilde{\rho}=\rho_2} = 0. \tag{13}$$

By expressing $U_{A2}|_{\tilde{\rho}=\rho_2}$, as defined by Eq. (13), in terms of the angle $\tilde{\varphi}$ and then expanding in Fourier series and setting the expansion coefficients to zero, the equations relating the U_{A2} coefficients to each other are obtained. These equations, together with the equations following from Eqs. (8), (9), and (12) define the coefficients of the potential expressions. The solution of these equations yields the potential distribution in all regions of the system and makes it possible to calculate the electrostatic field strength in any region.

The results of the calculations of electrostatic field strength in the region between the toner and the paper in this case are shown in Figs. 5 and 6. The conditions for the photoreceptor and toner charges are the same as in case A.

CALCULATION RESULTS AND ANALYSIS OF ELECTRIC FIELD DISTRIBUTION

The solution of the system of equations for the determination of the coefficients in the expressions for the potential (see the explanation after Eqs. (8) and (10)) involves the replacement of an infinite series by a finite series for each region (toner, air, paper, etc.), with the same number N of unknown coefficients N has been chosen based on the requirement that an increase in N does not lead to a change in the first three significant digits of the calculated electric field.

The development of the method for the accurate calculation of the electric field in the toner image transfer system makes it possible to compare similar calculations in 1D and 2D for various geometries of the toner image transfer module and for various paper parameters—thickness and dielectric permittivity. First, we consider the limiting case, when the toner transfer element is flat. This is similar to the case when the toner image is transferred by applying a corona discharge to the paper. In this case, the results of calculations of the vertical component E_x of the electric field using the dielectric thickness approximation, which were obtained earlier,[8] and the present results, which have been obtained by characterizing the paper more accurately by thickness and dielectric permittivity separately, are compared in Figure 3. It is evident that, when the paper dielectric thickness is sufficiently small ($d / \varepsilon_p = 0.0005$, Fig. 3(a), curves 1, 4, 5), the results obtained by the two methods coincide. As the dielectric thickness increases (Fig. 3, curves 2, 6, 7 when $d / \varepsilon_p = 0.002$ and curves 3, 8, 9 when $d / \varepsilon_p = 0.0033$), the difference between the results obtained by the two methods increases, and this difference becomes more pronounced at larger ε_p (in agreement with Ref. 6). When $\varepsilon_p = 20$, the difference in the E_x values in the interval $0 \le y \le 0.05$ is still less than 5 %, and it is even smaller for larger values of y. Since the cylinder radius is 1 to 1.5 cm, the values $\varepsilon_p = 20$ and $d / \varepsilon_p = 0.002$ correspond to a paper thickness of 400 – 600 μm. The true paper thickness and dielectric permittivity (the maximal value reported[16] for coated paper is 15) are smaller than those values, so that, at the same value of ε_p, the paper dielectric thickness is less. In the case of paperboards (thickness 400–600 μm), the dielectric thickness is also less because the dielectric permittivity does not exceed 10. The differences in the results are thus smaller than those shown by curves 2 and 6. Thus, we may conclude that when ε_p does not exceed 20 the vertical component E_x of the electric field strength in the air between the toner and the paper, and hence the calculated conditions for the Paschen effect, can be expressed with sufficient accuracy via the paper dielectric thickness d / ε_p, rather than via the paper thickness d and dielectric permittivity ε_p separately.

The dependence of the vertical electric field component E_x on the paper thickness at various dielectric permittivities has been investigated (Fig. 4(a)). E_x increased with increasing dielectric permittivity and decreased with increasing distance from the point where the paper was in contact with the toner ($y = 0$). It should be noted that the dependence of the vertical electric field component on the paper thickness depends on the dielectric permittivity of the paper (Fig. 4(a)). The shape of the curves corresponds to the transition from $\varepsilon_p = \varepsilon_0$ (Fig. 4(a), curve 1), when $E_x \sim d^{-1}$ (if $d > d_{smicond} + d_{toner}$), to $\varepsilon_p = \infty$ (Fig. 4(a), curve 7) when E_x does not depend on the paper thickness d, as expected. The dependence of E_x is shown in Fig. 4(a) at the coordinate $y = 0.15$, i. e., at the distance that is

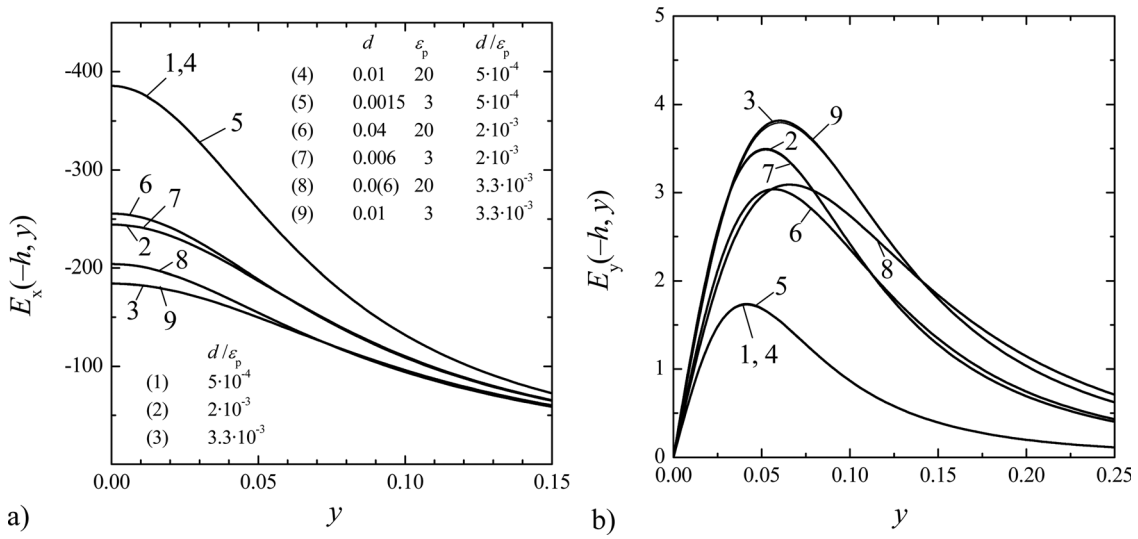

Figure 3. The electric field strength in the units U_o (V)/R(cm) on the paper surface when the toner image transfer element is flat: a—the component perpendicular to the paper, b—the horizontal component. 1–3: the dielectric thickness approximation for the paper (according to Ref. 8); 4–7: results when the paper is characterized by its thickness d and dielectric permittivity separately. The semiconductor and toner dielectric permittivities were 2 and 2.5, respectively, and their dimensionless thicknesses were 0.001 and 0.004, respectively; the dimensionless density of the toner space charge was $Q = 200$. The coordinate y and the values of the thickness are expressed in units of the photoreceptor cylinder radius R.

important both for image transfer and for the Paschen effect (Fig. 7), and the dependence of E_y is shown at $y = 0.05$, where E_y is equal to the maximum value.

In the case of a flat toner transfer element, there was no difference between the value of the horizontal component E_y calculated using the dielectric thickness approximation and the value calculated exactly if the dielectric thickness was sufficiently small (d / $\varepsilon_p = 0.0005$, Fig. 3(b), curves 1, 4, 5). However, when the dielectric thickness was increased, the difference became more pronounced (Fig. 3(b), curves 2, 6, 7 when d / $\varepsilon_p = 0.002$, and curves 8, 9). The horizontal componenst E_y is equal to zero at the point of contact between the paper and the toner ($y = 0$). As the distance from this point increases, the horizontal component increases and reaches a maximum at approximately $y = 0.5$ and then decreases continuously. However, within the practically important region $0 \le y \le 0.15$, the maximum values of E_y are relatively small, comprising only 1 – 2 % of the magnitude of the vertical component E_x. When the paper thickness is varied, the horizontal

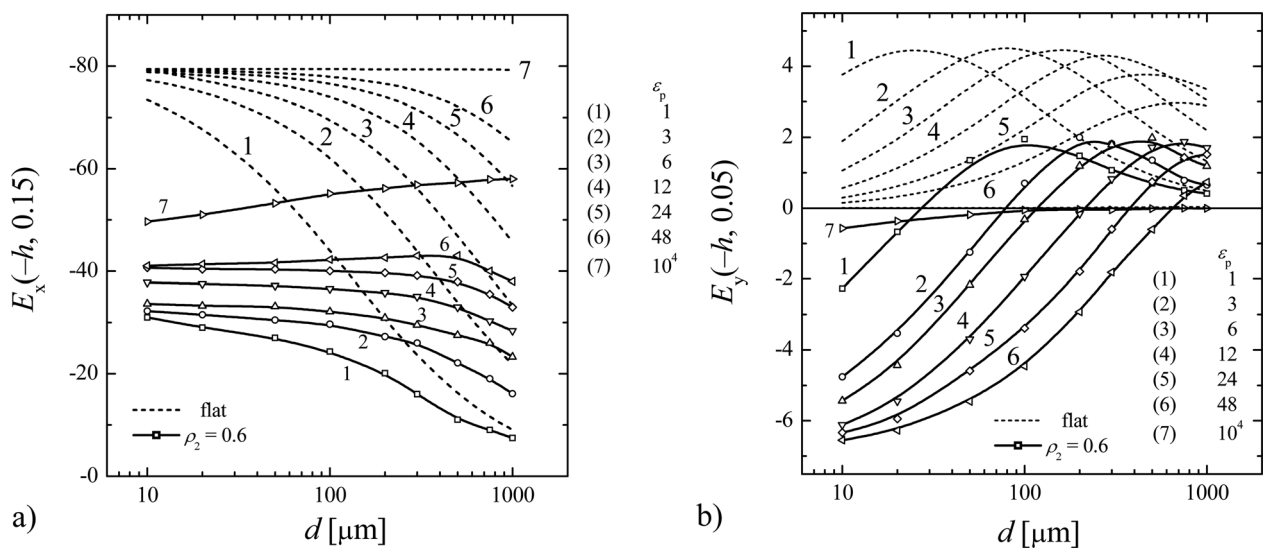

Figure 4. Dependence of the electric field components in units U_o (V)/R(cm) on the paper thickness at different values of its dielectric permittivity ε_p. The semiconductor and toner dielectric permittivities are 2 and 2.5, their dimensionless thicknesses were 0.001 and 0.004, respectively; $U = 1000$ V; transfer roller radius was 0.6; $Q = 200$. The values of the semiconductor and toner thickness and radius of the transfer roller are expressed in units of the photoreceptor cylinder radius R.

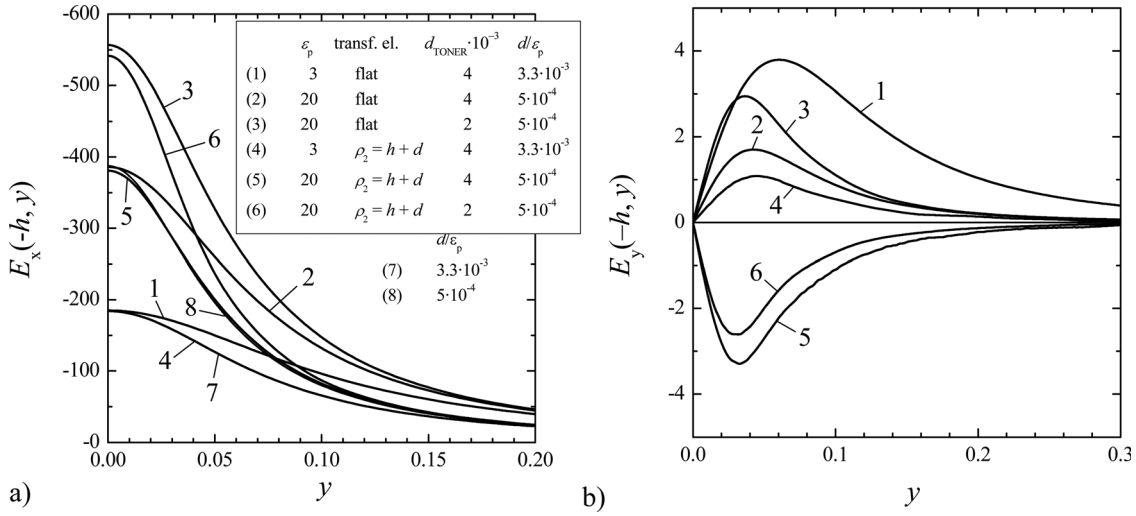

Figure 5. The electric field components on the paper surface: a—the component perpendicular to the surface; b—the component parallel to the surface. The transfer element is a roller with finite radius (curves 4–6), flat (curves 1–3). Curves 7 and 8 correspond to the dielectric thickness approximation for the paper in the case of a finite-radius element. In all cases, the semiconductor dimensionless thickness is 0.001, and $\varepsilon_2 = 2$; the paper dimensionless thickness is 0.01, and $\varepsilon_2 = 2.5$. The values of the coordinate y and the thickness are expressed in units of the cylinder radius R, and the electric field strength is expressed in units of U_0/R.

component attains the maximum value, and when the paper dielectric permittivity is varied, the maximum shifts towards increasing paper thickness (Fig. 4(b)).

It should be noted that the dielectric thickness approximation for the paper when calculating the E_x component is also valid for the roller. For example, see curves 7 and 8 in Fig. 5(a) for the case $\rho_2 = h + d$, and in the case $\rho_2 = 0.6$ the difference between the parameters of Fig. 5 does not exceed 3 % for all y values. The calculation results indicate in the case of the parameters of Fig. 5 that the dielectric thickness approximation is also valid for the toner. For example, when $d = 0.01$, $\varepsilon_p = 3$, $\rho_2 = h + d$ and $d_{TONER} = 0.004$, $\varepsilon_{TONER} = 2.5$, we obtain $E_x(-h, 0.05) = 126.66$, and when $d_{TONER} = 0.008$ and $\varepsilon_{TONER} = 5$ (i. e., $(d/\varepsilon)_{TONER} = 1.6\cdot10^{-3}$ in both cases), we obtain $E_x(-h, 0.05) = 125.21$. The difference in the electric field values at the chosen point $(-h, 0.05)$ is only 1.16 %.

The results of calculations for the case of a transfer roller, when the paper is characterized separately by its thickness and dielectric permittivity, compared with the case of a flat toner image transfer element are shown in Figs. 5 and 6.

These graphs indicate that, when the roller radius does not exceed $h + d$, the perpendicular component E_x of the

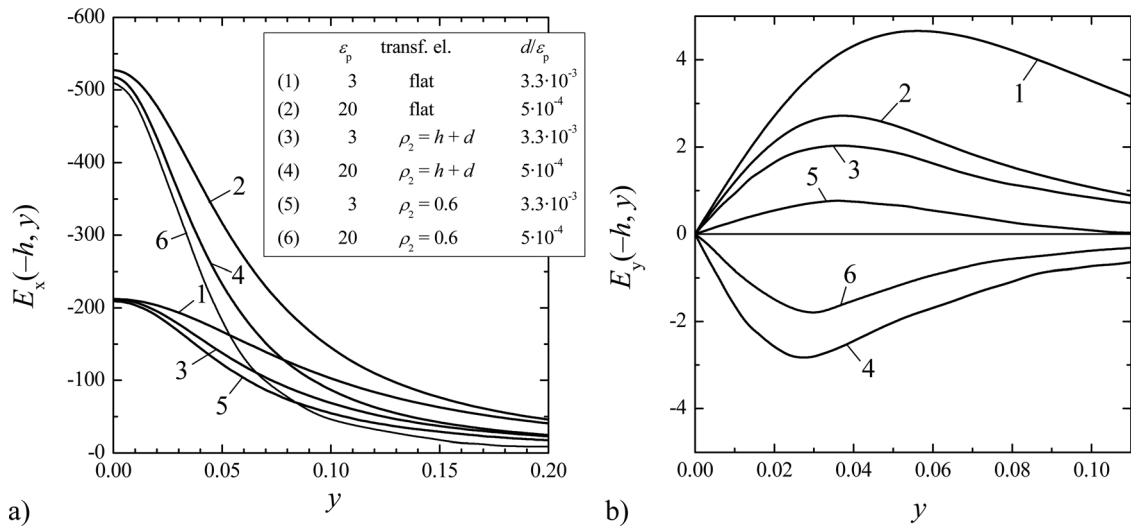

Figure 6. The electric field components on the paper surface: a—the component perpendicular to the surface; b—the component parallel to the surface. The paper transporter is a finite-radius roller (curves 3–6), flat (curves 1 and 2). In all cases the semiconductor dimensionless thickness is 0.002 and $\varepsilon_2 = 2$; the toner dimensionless thickness is 0.001; $Q = 200$. The coordinate y and the values of the thickness are expressed in units of the cylinder radius R, and the values of electric field strength are expressed in units of U_0/R.

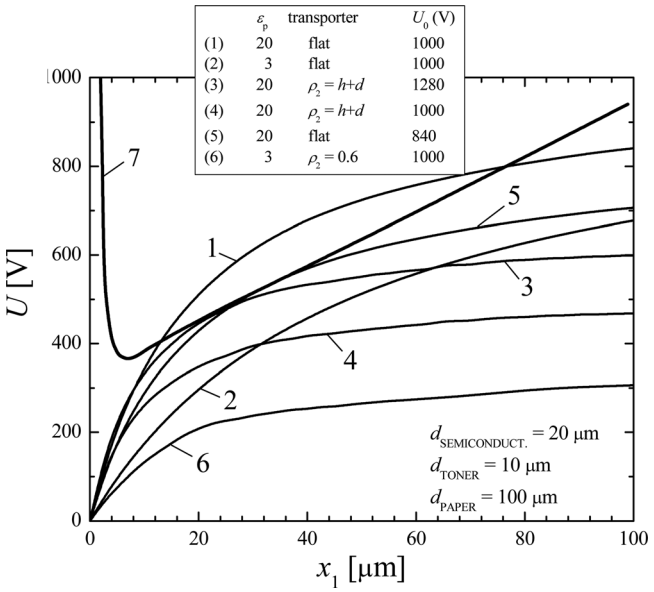

Figure 7. The Paschen effect: curves 1 to 6—calculated dependence of potential change in the layer of air on the thickness x_1 of that layer, when the cylinder radius is 1 cm, semiconductor and toner dielectric permittivities: $\varepsilon_1 = 2$ and $\varepsilon_2 = 2.5$; $Q = 200$; 7—Paschen curve.[17]

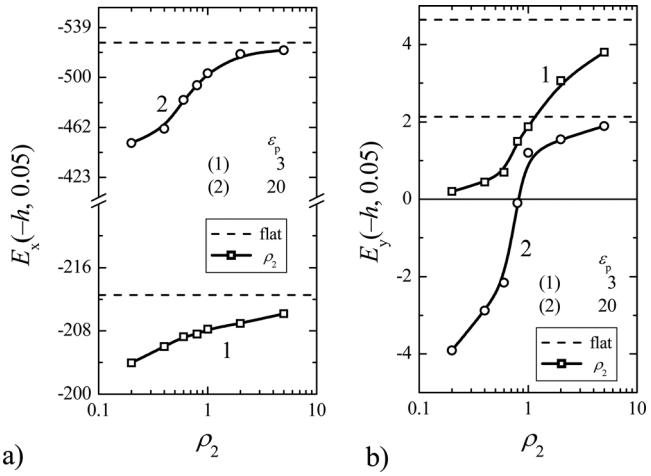

Figure 8. Dependence of the electric field components on the dimensionless radius of the transfer roller. The paper thickness was 0.01, and the other parameters are the same as in Fig. 4. The transfer roller radius is expressed in units of the photoreceptor cylinder radius R.

electric field is less than the value of E_x in the case of a flat transporter. If the difference between the field values at the point of contact of the paper and the toner ($y = 0$) corresponding to the cases of a flat transfer element and a cylinder-shaped transfer element is insignificant (although it increases with increasing dielectric permittivity), the mentioned difference increases rapidly and becomes significant with increasing distance from that point. The physical reason is understandable: when the roller radius ρ_2 is finite, the distance between the electrodes in the x-direction corresponding to a given value of y is greater than in the case of a flat transfer element, e.g., when $\varepsilon_p = 20$ (Fig. 5, curves 3, 6 and 2, 5; Fig. 6, curves 2, 4), the E_x values for the case $\rho_2 = h + d$ at $y = 0.1$ are only about 60 % of the E_x values for the case of a flat transporter. As ρ_2 decreases, this ratio becomes even smaller (Fig. 6). The relative decrease in the calculated potential required for the Paschen effect is approximately the same (Fig. 7). For example, if in the case of a flat transporter at $U_0 = 1000$ V, $\varepsilon_p = 20$ (Fig. 7, curve 1) the Paschen effect is possible in the interval $0.05 \leq y \leq 0.12$, then at $\rho_2 = h + d$ the value of U_0 required for the Paschen effect becomes greater than 1280 V (Fig. 7, curve 3), and at $\rho_2 = 0.6$ even larger U_0 values are obtained (cf. curves 2 and 6 in Fig. 7). Bearing in mind that, in the case of a flat transporter, the electric components in the air between the toner and the paper are similar to the values obtained by applying the 1D model to the image transfer system,[8] it follows that, when the toner image is transferred by a roller whose radius does not exceed the cylinder radius, the 1D model is not applicable for the description of the image transfer dynamics and for the prediction of the Paschen effect.

This technique of electric field calculation makes it possible to evaluate relatively easily the electric field strength at various geometries of the transfer nip and various paper thicknesses and dielectric permittivities. The results obtained using this method show the dependence of the vertical and horizontal components of the electric field on the paper thickness for various values of the paper dielectric permittivity (Fig. 4) and the dependence on the transfer roller radius (Fig. 8).

In the case of a flat transfer element, the horizontal electric field component E_y on the paper surface is always positive (Figs. 4 and 8), and it thus defocuses the charge. When ρ_2 is finite, a change in ε_p (or in d) can cause a change in the sign of E_y, so that it begins to focus the transferred toner image (Fig. 4(b), curves 4, 5, Fig. 5(b), curves 3, 4, Fig. 8). At a particular value of ε_p, the horizontal component can become zero. The calculation gives, that in the case of parameter values of Fig. 4(b), E_y vanished when $\varepsilon_p = 5.1$, and when the semiconductor, toner and paper thicknesses were 0.002, 0.001, and 0.01, respectively, E_y vanished when $\varepsilon_p = 7.8$. The horizontal electric field component also depends on the diameter of the transfer roller and on the paper dielectric thickness (Fig. 8).

CONCLUSIONS

The electrostatic field distribution in any part (finite or infinite) of the toner image transfer system can be calculated with the required precision by expanding the solution of the Poisson equation for the potential in terms of partial solutions satisfying the real boundary conditions of the corresponding region in the toner image transfer nip (paper, air, toner). This technique makes it possible to complete the calculations in a relatively small number of steps and thus to decrease the requirements for the computing system compared with the finite-difference method. The calculation of the electric field strengths and their distribution in the toner image transfer nip has made it possible to evaluate the limits of applicability of the 1D approximation and to determine peculiarities of electric field distribution at various transfer nip geometries and for different sets of paper parameters.

When the radius of the paper-transporting roller is close to or less than the photoreceptor radius, the 1D approximation cannot be used to calculate the electric field strength in the region between the toner and the paper.

The results of calculations of electric field in the toner image transfer nip have revealed some peculiarities. It has been shown that the electric field strength depends on the paper thickness and its dielectric permittivity, but that it is almost independent of the transfer nip geometry. However, the character of the variation of the vertical component with increasing distance from the point of contact between the paper and the toner is markedly affected by the transfer nip geometry. Since the electric field in this region can also influence the quality of the transferred image, this peculiarity should be taken into account in the design of the equipment, and appropriate adjustments should be applied, for example, when the paper thickness is changed, i.e., when the paper is replaced.

Although the horizontal electric field component is small, it is markedly dependent on the transfer nip geometry, and on the paper thickness and dielectric permittivity. When the toner image is transferred to the paper by a roller, the sign of the horizontal component can change depending on the conditions. Under certain conditions, which depend on the paper thickness and its dielectric permittivity, the electric field component parallel to the paper surface becomes zero. When these conditions have passed, the sign of the component changes (Figs. 4(b), 5(b), and 8).

The calculation procedure developed in this work can also be used in the investigation of other factors affecting the electric fields in the nip region e.g. sheet transfer in the nip.

ACKNOWLEDGMENTS

Dr. Anthony Bristow is thanked for the linguistic revision of the manuscript.

REFERENCES

[1] J. Kallunki, M. Alava, and E. K. O. Hellen, "The electric field close to an undulating interface", J. Appl. Phys. **100**, 023528 (2006).
[2] A. Cassidy, M. Grant, and N. Provatas, Model. Simul. Mater. Sci. Eng. **12**, 91 (2004).
[3] Ch. Tong, T. Wu, and N. Provatas, Model. Simul. Mater. Sci. Eng. **14**, 1447 (2006).
[4] P. Sirviö and K. Backfolk, "Effect of roughness of low-grammage coated papers on print quality in color electrophotography", J. Imaging Sci. Technol. **51**, 010505 (2008).
[5] M. Schleusener, *Proc. IS&T's NIP7: Int. Congress on Advances in Non-Impact Printing Technologies* (IS&T, Springfield, VA, 1991), p. 167.
[6] T. N. Tombs, *Proc. IS&T's NIP14: Int. Conf. Digital Printing Technologies* (IS&T, Springfield, VA, 1998), p. 440.
[7] Y. Furuya, J. Imaging Sci. Technol. **45**, 542 (2001).
[8] J. Kaladė, R. Maldžius, J. Sidaravičius, P. Sirviö, and K. Backfolk, "Dependence of electrostatic field on properties of paper in a two-dimensional toner image transfer nip", Lith. J. Phys. **49**, 145 (2009).
[9] M. Kadonaga, "2-dimensional electrical simulation of electrostatic transfer process using discreteelement method", *Proc. Japan Hardcopy 2001* (Imaging Society of Japan, Tokyo, 2001) [in Japanese].
[10] T. Sasaki, S. Nasu, T. Nakaegawa, M. Saito, and J. Asai, *Proc. Japan Hardcopy, 2004* (Imaging Society of Japan, Tokyo, 2004) [in Japanese].
[11] Sh. Aoki, M. Sukesaki, and M. Kadonaga, "A numerical simulation method of toner transfer considering voltage distribution of transfer belt", *Proc. IS&T's NIP23: Int. Conf. on Digital Printing Technologies and Digital Fabrication* (IS&T, Springfield, VA , 2007), pp. 77–80.
[12] T. Sasaki, K. Yamamoto, T. Onishi, A. Sugiyama, T. Tomizawa, and Y. Yoda, "Sheet transport simulation for electrostatic transfer process in electrophotography", J. Imaging Sci. Technol. **54**, 030504 (2010).
[13] T. Sasaki, T. Onishi, A. Sugiyama, S. Nasu, Y. Yoda, and T. Tomizawa, "Transfer process multiphysics simulation in electrophotography", J. Imaging Sci. Technol. **54**, 030504 (2010).
[14] M. Katonaga, T. Katoh, T. Takahashi, and Y. Kishi, "Numerical simulation of separating discharge in the belt transfer system", J. Imaging Sci. Technol. **45**, 547 (2001).
[15] N. Leoni, "Numerical Simulation of Townsend Discharge, Paschen Breakdown and Dielectric Barrier Discharges", *Proc. IS&T's NIP25: Int. Conf. on Digital Printing Technologies and Digital Fabrication* (IS&T, Springfield, VA, 2009), p. 229.
[16] S. Simula, "Electrical Properties of Digital Printing Papers", "Advances in Printing Science and Technology. Advances in Digital Printing", *Proc. 26th Research Conference International. Association of Research Institute, Printing, Information and Communication Industries* (Pira International Ltd., Munich, 1999).
[17] R. M. Schaffert, *Electrophotography*, 2nd ed. (Wiley, New York, 1975), p. 989.